

# Slip on an active wedge thrust from geodetic observations of the 8 October 2005 Kashmir earthquake

Rebecca Bendick University of Montana, Department of Geosciences, Missoula, Montana 59812-1296, USA

Roger Bilham University of Colorado, Department of Geological Sciences, 399 UCB, Boulder, Colorado 80309-0399, USA

M. Asif Khan

S. Faisal Khan

University of Peshawar, National Centre of Excellence in Geology, Peshawar, NWFP 20005, Pakistan

## ABSTRACT

By combining global positioning system observations of surface displacements and the locations of aftershocks, we infer that the 8 October 2005 Kashmir earthquake occurred on multiple fault planes. Mean slip of  $\sim 5.1$  m occurred on a rupture between Bagh and Balakot with strike  $331^\circ$  and dip  $29^\circ$ . Additional slip occurred at depth on a NNE-dipping fault plane extending WNW from Balakot, and on an intersecting nearly flat dislocation at  $\sim 5$  km depth, forming an active wedge thrust. Both the simple fault plane and the blind wedge accommodate convergence between Peshawar and Leh, Ladakh, accumulating at  $7 \pm 2$  mm/yr, suggesting a  $680 \pm 150$  yr recurrence interval for Kashmir 2005-like events.

**Keywords:** Kashmir earthquake, wedge thrust, Himalayan tectonics.

## HISTORIC AND TECTONIC SETTING

The 8 October 2005 earthquake ruptured the westernmost end of the Himalayan arc between the site of the 28 December 1974 Pattan earthquake (Ambraseys, 1975; Pennington, 1979; Jackson and Yielding, 1983) and sites of damaging earthquakes to the southeast that occurred in 1555 and 1885 (Iyengar et al., 1999). The mapped surface rupture partly follows the Kashmir Boundary Thrust on the western margin of the Hazara syntaxis (Armbruster et al., 1978) where it bends around the western syntaxis, as well as a splay to the southeast (Geological Survey of Pakistan, 2004). However, global positioning system (GPS) and aftershock observations also require slip on 8 October 2005 and afterward within the Indus-Kohistan seismic zone, on a blind thrust below a flat décollement at  $\sim 5$  km depth, extending WNW from the Main Boundary Thrust (Fig. 1). We use GPS, aftershocks, and focal mechanisms to constrain dislocation models of rupture geometry and slip for the Kashmir event.

A SW-facing wedge thrust was first inferred in the Indus-Kohistan seismic zone from microseismicity (Seeber and Armbruster, 1979) (Fig. 1). Similar arrangements of intersecting fault planes, called wedge thrusts, are exposed in inactive continental collisions, including the Canadian Rockies (Stockmal et al., 2001) and the Pyrenees (Beaumont et al., 2000), and in active collision zones including the Seattle uplift (Brocher et al., 2004) and the Kirthar and Sulaiman Ranges (Banks and Warburton, 1986), although coseismic slip on both fault planes of an active wedge thrust has not previously been observed. The critical element in generating and maintaining slip on the passive-roof décollement of a wedge thrust is an extremely weak crustal layer (Couzens-Schultz et al., 2003). In the Balakot-Pattan region, this layer probably consists of weak Precambrian

to Ordovician black shales and evaporite layers (Bossart et al., 1988).

The history of Kashmir shows that the region, in common with the entire Himalaya, regularly experiences moderate earthquakes, but infrequently damaging ones (Fig. 2). An especially long historical record of earthquakes is available because of the stability of the administrative center at Srinagar. Additional early data have been obtained from Urdu and Arabic histories (Iyengar and Sharma, 1999). Earthquakes of various degrees of severity were felt in Srinagar in 883, 1123, 1501, 1555, 1669, 1736, 1779, and 1784 (Iyengar et al., 1999). More recent earthquakes in 1828 (Vigne, 1842), 1885 (Jones, 1885a, 1885b; Lawrence, 1895), and 1974 (Jackson and Yielding, 1983) are well described, but only for the last two are the construction of isoseismal maps possible. The September 1555 earthquake damaged a 200-km-long region from near Srinagar to the southeast (Iyengar et al., 1999) and has been assigned  $M_s = 7.6$  (Ambraseys and Douglas, 2004). The inferred rupture zone based on these accounts is at least twice as long as the 2005 event, but low historical population density in the Pir Panjal produces uncertainty about the southeast extent of the 1555 rupture. Either a significant seismic gap persists to its southeast or the 1555 earthquake may have been  $M_w \geq 8$ .

## 2005 OBSERVATIONS

The NEIC (National Earthquake Information Center), USGS (U.S. Geological Survey), and Harvard CMT (Centroid-Moment Tensor) solutions for the 8 October 2005 Kashmir event indicate a NW-SE-striking rupture plane, with dips ranging from  $29^\circ$  to  $40^\circ$ . Waveform inversions by Parsons et al. (2006) and Avouac et al. (2006) give strike, dip, and rake of  $331^\circ$ ,  $31^\circ$ , and  $108^\circ$ , and  $325^\circ$ ,  $29^\circ$ , and  $110^\circ$  respectively. SAR (synthetic aperture radar) inversion indicates rupture

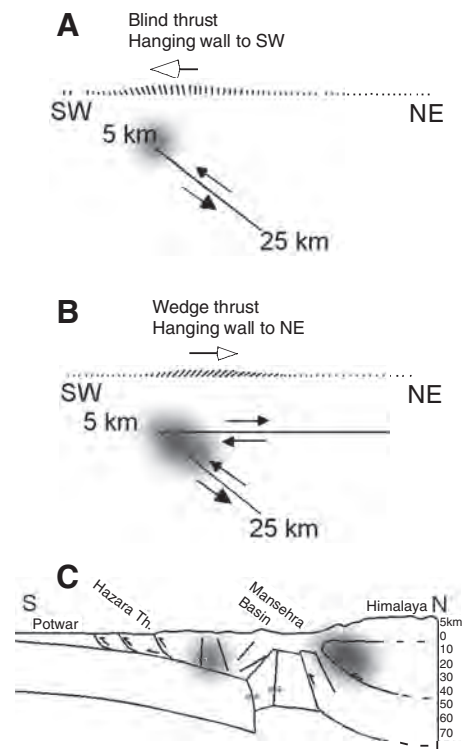


**Figure 1.** Surface horizontal displacements differ in sign between simple blind thrusts (A) and wedge thrusts (B). Shaded areas indicate stress concentrations and large numbers of aftershocks. Part of the 8 October 2005 Kashmir earthquake appears to have occurred on a wedge thrust in the Indus-Kohistan seismic zone mapped by Seeber and Armbruster (1979) (C).

on an 80-km-long fault of strike  $321.5^\circ$  and dip  $31.5^\circ$  (Pathier et al., 2006), with maximum slip near Balakot, as in the Parsons et al. (2006) solution. The main rupture reaches the surface in several places. Additional, primarily vertical, displacement is observed beyond the northwest end of the main rupture (Pathier et al., 2006).

The moment release in aftershocks is only a few percent of that released by the main shock, but their location and number indicate a complexity inconsistent with a planar rupture or even the slightly concave-NE rupture of Avouac et al. (2006). More than 75% of the aftershocks occur in a cluster  $\sim 30$  km southwest of the strike of the main rupture, along a more westerly trend within the Indus-Kohistan seismic zone (Seeber et al., 1980) (Fig. 3). Aftershocks in this clus-

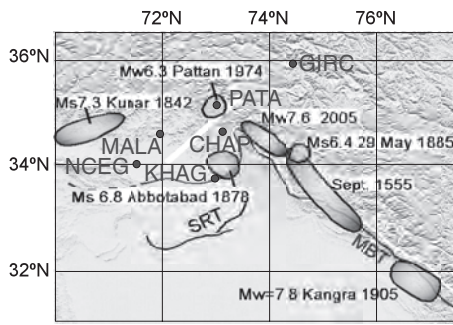


**Figure 2. Historical locations reporting MSK-64 shaking intensities exceeding VII for earthquakes in the past 500 yr (Ambraseys and Douglas, 2004). The inferred rupture zone for 1555 is shifted southeast of the reports to account for a possible reporting bias caused by populations in the Kashmir Valley. Black circles with four-letter codes indicate points with pre- and postseismic GPS observations. The white line is the location of the Seeber and Armbruster (1979) cross section in Figure 1. MBT—Main Boundary Thrust; SRT—Salt Range Thrust.**

ter with sufficient moment for depth and focal mechanism inversions indicate slip on a plane with dip comparable to the main rupture plane, but much shallower than the hypocenter of the main shock (Fig. 4).

A sparse array of geodetic monuments was installed and measured in June 2001 in the epicentral region (Fig. 2) and remeasured in October and November 2005, beginning three weeks after the main rupture. Because pre-seismic observations of these points were made at only one epoch, we are able to calculate only the total displacement of the points over the period 2001–2005. We assume that this sparse displacement field is dominated by the coseismic signal, and model it, below, solely with instantaneous slip on a set of elastic dislocations whose geometry is constrained by the focal mechanisms, seismic waveform inversions, and aftershock observations.

Geodetic GPS data were logged at 30 s intervals during both 2001 and 2005 (Table 1), using Trimble 5700 receivers and Trimble Zephyr Geodetic antennas. These data were processed at the University of Montana, using GAMIT/GLOBK (Herring, 2002). Additional IGS (International GNSS Service) stations were added to the regional network, as were two stations in Ladakh, India. We calculated final velocity solutions in the ITRF00 reference frame by including position and velocity data for the entire IGS network from SOPAC (Scripps Orbital and Permanent Array Center). We also calculated the velocity of sites in Pakistan relative to Ladakh by estimating an angular velocity vector between ITRF00 and the Ladakh sites. This velocity solution agrees with a frame-independent scalar estimate of shortening between Peshawar and Ladakh, calculated by fitting a linear trend to the time series of baseline length between Peshawar

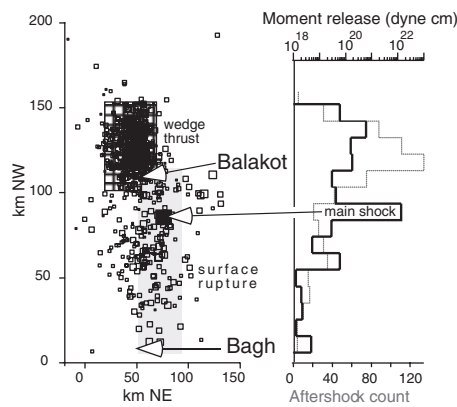


**Figure 3. Aftershocks reported by NEIC plotted as a function of transverse and longitudinal distance along the rupture to illustrate the offset between the surface rupture and the knot of aftershocks at its northwest end. The region corresponds to Indus-Kohistan seismic zone, and 75% of all aftershocks occur there and release ~3% of the total main shock moment release. Aftershock moment (black line), and numbers of events (gray line) are summed in 10 km segments along strike.**

and Ladakh. Uncertainties in position and velocity reflect the scatter in daily solutions about the best-fit values, as well as a random-walk component. We calculated the displacement vectors for sites within 150 km of the 8 October 2005 epicenter by solving for the preseismic-postseismic baseline components. We assume in the following models that this baseline represents instantaneous surface displacement caused by subsurface rupture.

Table 1 provides the position, velocity (in several reference frames), and horizontal coseismic displacement vectors for all sites with pre- and postseismic observations. Stations within 150 km of the epicenter have only coseismic displacement estimates; stations beyond that radius have only velocity estimates.

The largest coseismic displacement,  $25.9 \pm 0.7$  cm (all uncertainties are  $1\sigma$ ), occurred at Chatter Plain (CHAP) at  $34.62^\circ\text{N}$ ,  $73.11^\circ\text{E}$ . This site is 44 km from the reported Harvard CMT epicenter at  $34.36^\circ\text{N}$ ,  $73.47^\circ\text{E}$ . CHAP is also 36 km from Balakot, the site of maximum slip in the SAR inversion (Pathier et al., 2006). Displacement of  $19.1 \pm 0.4$  cm occurred at Kantla village (KHAG) near Taxila, 85 km nearly due south of the epicenter. Significant displacement,  $7 \pm 0.7$  cm, was also recorded at Pattan (PATA), north of the epicenter, close to the trace of the 1974 Pattan earthquake (Fig. 4).

The velocity of Peshawar relative to Ladakh, India, is  $9.8 \pm 1.3$  mm/yr, with a component of  $8.6 \pm 2$  mm/yr normal to Himalayan thrusts striking  $\sim 330^\circ$ . This convergent component of velocity agrees with the rate of baseline shortening between Peshawar and Hanle, Ladakh, of  $6.2 \pm 1.5$  mm/yr ( $1\sigma$ ) from the daily baseline length

time series. There is therefore very little shear in the western Himalaya, despite the obliquity of the range to the India-Asia convergence direction.

## KINEMATIC MODEL

While planar dislocation models such as those from waveform or radar inversions (Parsons et al., 2006; Avouac et al., 2006; Pathier et al., 2006) are consistent with coseismic GPS displacements at CHAP and KHAG, we are unable to reproduce even the sign of observed displacement at PATA, or explain the unusual distribution of aftershocks with this simple dislocation geometry (Fig. 4). A fault model combining the main rupture with a wedge thrust based on historical regional seismicity (Seeber and Armbruster, 1979), aftershock distributions, and aftershock focal mechanisms is successful in emulating slip at all three geodetic sites (Fig. 4). Most of the moment in this preferred rupture model is released as  $\sim 5.1$  m mean slip on the observed surface fault between Bagh and Balakot, with an additional 1.8 m of slip on the dipping plane of the wedge thrust in the northwest, and centimeters of slip on parts of the weak, flat-roof décollement. The presence of a wedge thrust is consistent with SAR observations of predominantly vertical displacement northwest of Balakot (Fig. 1) (Pathier et al., 2006). Dislocation parameters for the preferred model are given in Table 2, and the locations of dipping and flat dislocations are shown in Figure 4. As in analog and numerical models of wedge thrusts (Couzens-Schultz et al., 2003; Beaumont et al., 2000) slip on the flat-roof décollement occurs in the opposite direction to slip on the dipping part of the wedge, and the magnitude of slip varies in space on the flat as the weak horizon slips in response only to the local stress.

The combination of décollement and reverse slip required by satisfactory models is extremely nonunique since the solution is undetermined by the surface displacement field alone (three vectors cannot constrain three to four planes, each with nine unknowns). However, because we have included a priori geometric constraints from other seismic and geodetic observations to build the model geometry, the GPS displacements are only used to constrain the magnitude of the slip vector. We cannot reproduce the direction of displacement at Pattan without either the wedge décollement (Seeber and Armbruster, 1979) or another undocumented fault to the northwest.

Coulomb stress (Toda et al., 1998) resulting from this rupture configuration is large and positive (for NE-dipping reverse slip) in a region southeast of the rupture. The postseismic Coulomb stress northwest of the rupture is much smaller in magnitude, although still positive. All models of the 8 October 2005 rupture predict large positive Coulomb stress changes to the southeast (Parsons et al., 2006), in a region that has not hosted a large rupture since 1555.

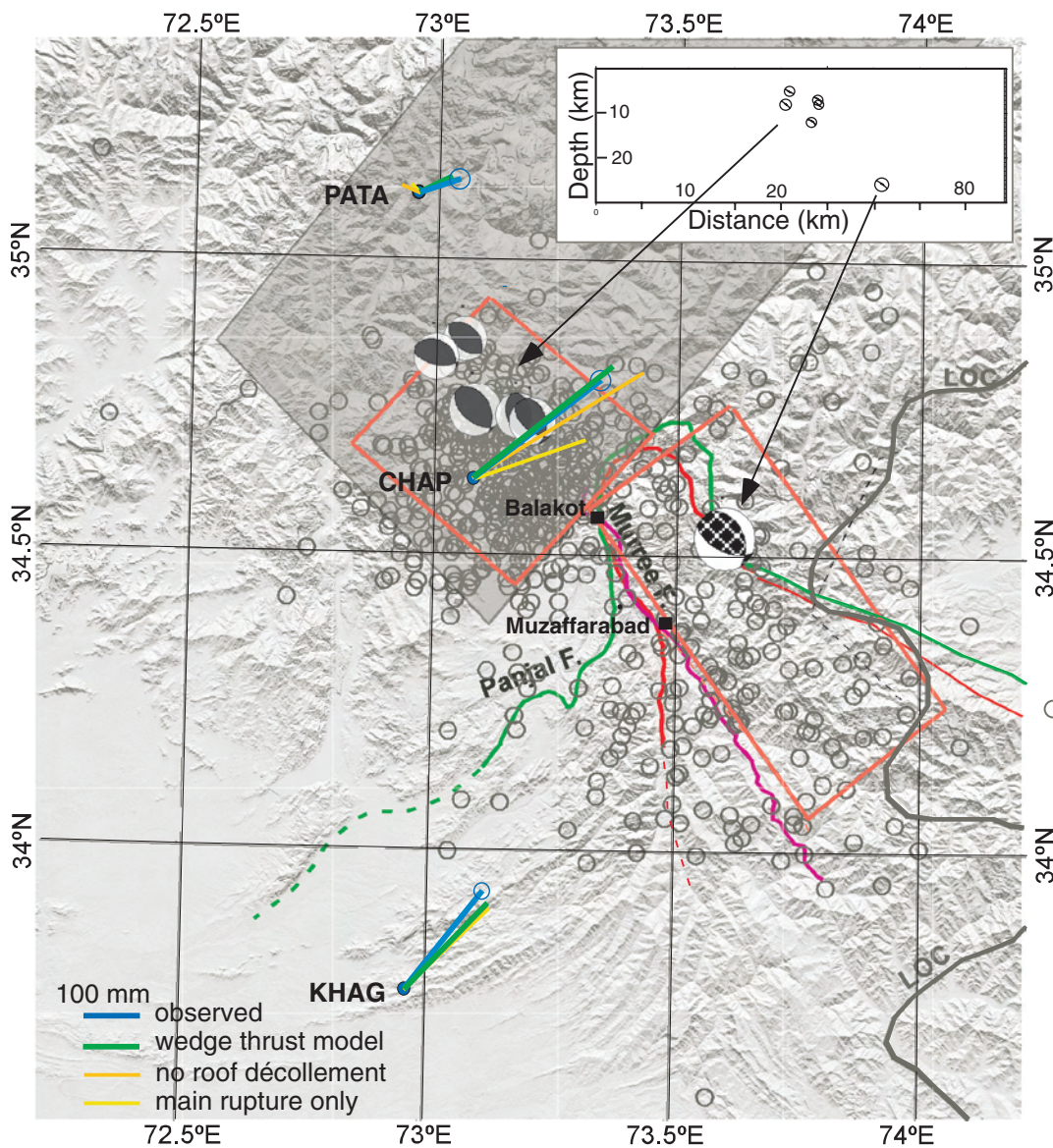


Figure 4. Observed and modeled displacements (for three different models) for the geodetic sites, aftershock distribution and mechanisms where available, and model geometry. Dipping dislocations are outlined in orange; the approximate extent of the flat-roof décollement is in gray (but poorly constrained). Recorded aftershocks are open gray circles; those with focal mechanisms are gray “beach balls.” The focal mechanism for the main rupture is the hatched beach ball. The mapped trace of the Main Boundary Thrust (locally the Murree fault) is red, the Main Central Thrust (locally the Panjal fault) is green, and the nodal plane from the radar range change is magenta. Inset: Focal mechanisms for the main shock and some aftershocks projected into a cross section normal to the strike of the main dislocation.

TABLE 1: DISPLACEMENTS AND VELOCITIES OF GPS SITES

Station	Latitude (°N)	Longitude (°E)	2001 Epochs	2003 Epochs	2005 Epochs	Coseismic N (mm)	Coseismic E (mm)	ITRF00 N (mm/yr)	ITRF00 E (mm/yr)	EURAN (mm/yr)	EURAE (mm/yr)	Ladakh N (mm/yr)	Ladakh E (mm/yr)
LHAS	29.657	91.104	078–234	160–230	335–338; 250–264			11.2 ± 0.5	35.3 ± 0.5	20.4 ± 1	23.3 ± 1	-5 ± 1	14.57 ± 1
IAOH	32.779	78.973	123–174	160–179; 200–289	314–329; 350–358			10.6 ± 0.8	15.7 ± 0.8	20.2 ± 1	5.1 ± 1	0.3 ± 1	0.5 ± 1
RSCL	34.128	77.6		160–233	355–359			12.1 ± 1	12.4 ± 1	21.6 ± 1	1.8 ± 1.3	1.6 ± 1	-1.6 ± 1
IISC	13.021	77.57	078–122; 208–234	160–230	314–338; 350–364			26.1 ± 0.8	39.5 ± 0.8	38.5 ± 1	27.2 ± 1	18.6 ± 1	11.7 ± 1
CHAP	34.617	73.106	193–198		314–318; 363	146 ± 7	213.9 ± 7						
PATA	35.112	72.998	193		323–327	30 ± 6	63.3 ± 7						
KHAG	33.736	72.96	199–200		319–322	143 ± 3	126.1 ± 5						
MALA	34.572	71.933	200–201		322–328	-7 ± 2	-5.8 ± 3						
BUTT	32.805	72.374		221–224	334–338	-7.3 ± 2	2.4 ± 2						
PATH	33.134	72.352		224–225	333–338	-2 ± 4	-2.9 ± 4						
NCEG	34.004	71.487	078–116; 132–157; 201–234	160–230				15.9 ± 1	17.8 ± 1	25.5 ± 1	7.3 ± 1	8.6 ± 1	4.8 ± 1

## DISCUSSION

The 8 October 2005 Kashmir earthquake appears to have ruptured the surface for ~100 km in a reverse fault with mean slip of ~5.1 m, and triggered slip of ~1.8 m on a blind wedge

thrust to its northwest. The total moment of this model is  $2.86 \times 10^{20} \text{ N} \cdot \text{m}$  (Table 2), similar to the Harvard CMT moment of  $2.94 \times 10^{20} \text{ N} \cdot \text{m}$ . GPS observations, aftershock distributions, and historical seismicity all suggest the presence of

an active blind wedge extending WNW from the Kashmir Main Boundary Thrust. We infer a sequence in which slip on the main thrust propagated onto a second thrust between Balakot and Pattan. Because this thrust terminates in an

TABLE 2: MODEL DISLOCATION PARAMETERS

	Latitude (°N)	Longitude (°E)	Length (km)	Depth (km)	Strike	Dip	Dip slip (m)	Strike slip (m)	Moment (Nm)	Notes
Main rupture	34.4	73.65	77	0–20	331°	29°	5.1	-0.1	2.4 x 10 <sup>20</sup>	From Parsons et al., 2006 and Pathier et al., 2006
Wedge thrust	34.7	73.1	44	5–20	319°	29°	1.8	0.0	3.2 x 10 <sup>19</sup>	Dipping part of wedge
flat 1	34.9	73.4	44	5	NA	0.1°	-0.3	-0.0	2 x 10 <sup>18</sup>	Wedge roof
flat 2	34.6	73	44	5	NA	0.1°	0.0	-0.05	3.3 x 10 <sup>17</sup>	Flat SW of wedge tip
flat 3	35	73	33	5	NA	0.1°	-0.1	0.11	9.3 x 10 <sup>17</sup>	Flat N of wedge

inferred weak horizontal sedimentary stratum, stress from the buried rupture produced slip on a roof décollement. Subsequent aftershocks are confined to the main rupture area and the dipping part of the wedge thrust.

Wedge thrusts are common in convergent continental settings but have not previously been recognized in coseismic geodetic data. The presence of complex fault geometry allows additional free parameters in models, such that horizontal surface displacements do not uniquely constrain dislocation geometry at depth, refuting a common assumption in tectonic geodesy. However, a combination of vertical and horizontal geodesy with independent seismic or structural data can provide sufficient constraint on the geometry of the two surfaces of the wedge.

Overall, interseismic strain accumulation in this region is dominated by compression normal to these regional thrusts, and therefore radial to the Himalayan arc, at 7–8 mm/yr. Very little shear appears to accumulate between the Peshawar basin and the Karakorum Range, supporting suggestions that the dominant regime in the western syntaxis is SW-NE-shortening, rather than right-lateral shear. Convergence rates in the western syntaxis are at least a factor of two smaller than in the central arc (e.g., Zhang et al., 2004), such that the recurrence interval for events such as that of 8 October 2005 is 530–720 yr. If the recurrence intervals of the 1555 and 2005 earthquakes are similar, the positive Coulomb stress from the recent event may have advanced the 1555 Himalayan segment south-east of the recent rupture close to failure.

#### ACKNOWLEDGMENTS

We thank Bob Engdahl and Eric Bergmann, who provided us with improved locations for the focal mechanisms shown, using the waveform-modeled refined depths of George Choy. The work was funded by National Science Foundation grant EAR-0229690.

#### REFERENCES CITED

Ambraseys, N.N., 1975, Studies of historical seismicity and tectonics: *Geodynamics Today* (Royal Society of London), p. 7–16.

Ambraseys, N., and Douglas, J., 2004, Magnitude calibration of north Indian earthquakes: *Geophysical Journal International*, v. 159, p. 165–206, doi: 10.1111/j.1365-246X.2004.02323.x.

Armbruster, J., Seeber, L., and Jacob, K., 1978, The northwestern termination of the Hima-

layan mountain front: Active tectonics from microearthquakes: *Journal of Geophysical Research*, B, Solid Earth and Planets, v. 83, p. 269–282.

Avouac, J.-P., Ayoub, F., Leprince, S., Konca, O., and Helmberger, D., 2006, Surface ruptures and rupture kinematics of the 2005, Mw 7.6 Kashmir earthquake from sub-pixel correlation of Aster images and seismic waveforms analysis: 100th Anniversary Earthquake Conference, San Francisco, California.

Banks, C., and Warburton, J., 1986, “Passive-roof” duplex geometry in the frontal structures of the Kirthar and Sulaiman mountain belts, Pakistan: *Journal of Structural Geology*, v. 8, p. 229–237, doi: 10.1016/0191-8141(86)90045-3.

Beaumont, C., Hamilton, J., and Fullsack, P., 2000, Factors controlling the Alpine evolution of the central Pyrenees inferred from a comparison of observations and geodynamic models: *Journal of Geophysical Research*, v. 105, p. 8121–8145, doi: 10.1029/1999JB900390.

Bossart, P., Dietrich, D., Greco, A., Ottiger, R., and Ramsay, J., 1988, The tectonic structure of the Hazara-Kashmir syntaxis, southern Himalayas, Pakistan: *Tectonics*, v. 7, no. 2, p. 273–297.

Brocher, T., Blakely, R., and Wells, R., 2004, Interpretation of the Seattle uplift, Washington, as a passive-roof duplex: *Bulletin of the Seismological Society of America*, v. 94, no. 4, p. 1379–1401, doi: 10.1785/012003190.

Couzens-Schultz, B., Vendeville, B., and Wiltschko, D., 2003, Duplex style and triangle zone formation: Insights from physical modeling: *Journal of Structural Geology*, v. 25, p. 1623–1644, doi: 10.1016/S0191-8141(03)00004-X.

Geological Survey of Pakistan, 2004, Geological map of the Nauseri area, District Muzaffarabad, AJK, Islamabad: Geological Survey of Pakistan, scale 1:50,000.

Herring, T., 2002, GLOBK: Global Kalman filter VLBI and GPS analysis program version 10.0: Cambridge, Massachusetts Institute of Technology, 94 p.

Iyengar, R., and Sharma, D., 1999, Some earthquakes of the Himalayan region from historical sources: *Journal of Himalayan Geology*, v. 20, no. 1, p. 81–85.

Iyengar, R., Sharma, D., and Siddiqui, J., 1999, 1999, Earthquake history of India in medieval times: *Indian Journal of History of Science*, v. 34, no. 3, p. 181.

Jackson, J., and Yielding, G., 1983, The seismicity of Kohistan, Pakistan: Source studies of the Hamran (1972.9.3), Darel (1981.9.12) and Patan (1974.12.28) earthquakes: *Tectonophysics*, v. 91, p. 15–28, doi: 10.1016/0040-1951(83)90055-0.

Jones, E., 1885a, Notes on the Kashmir earthquake of 30th May 1885: Records of the Geological Survey of India, v. 18, no. 3, p. 153–155.

Jones, E., 1885b, Report on the Kashmir earthquake of 30th May 1885: Records of the Geological Survey of India, v. 18, no. 4, p. 221–227.

Lawrence, W., 1895, The Valley of Kashmir: London, H. Frowde, 478 p.

Parsons, T., Yeats, R., Yagi, Y., and Hussain, A., 2006, Static stress change from the 8 October 2005 M = 7.6 Kashmir earthquake: *Geophysical Research Letters*, v. 33, L06304, doi: 10.1029/2005GL025429.

Pathier E., Fielding, E., Wright, T., Walker, R., Parsons, B., and Hensley, S., 2006, Displacement field and slip distribution of the 2005 Kashmir earthquake from SAR imagery: *Geophysical Research Letters*, v. 33, L20310, doi: 10.1029/2006GL027193.

Pennington, W., 1979, A summary of field and seismic observations of the Pattan earthquake—28 December 1974, in Farah, A., and DeJong, K., eds., *Geodynamics of Pakistan: Quetta, Geological Survey of Pakistan*, p. 143–148.

Seeber, L., and Armbruster, J., 1979, Seismicity of the Hazara arc in northern Pakistan: Décollement vs. basement faulting, in Farah, A., and DeJong, K., eds., *Geodynamics of Pakistan: Quetta, Geological Survey of Pakistan*, p. 131–142.

Seeber, L., Armbruster, J., and Farhatullah, S., 1980, Seismic activity at the Tarbela Dam site and surrounding region: *Geological Bulletin of the University of Peshawar*, v. 13, p. 169–190.

Stockmal, G., Lebel, D., McMechan, M., and MacKay, P., 2001, Structural style and evolution of the triangle zone and external foothills, southwestern Alberta: Implication for thin-skinned thrust-and-fold belt mechanics: *Bulletin of Canadian Petroleum Geology*, v. 49, no. 4, p. 472–496, doi: 10.2113/49.4.472.

Toda, S., Stein, R., Reasenber, P., and Dieterich, J., 1998, Stress transferred by the 1995 Mw = 6.9 Kobe, Japan, shock: Effect on aftershocks and future earthquake probabilities: *Journal of Geophysical Research*, v. 103, p. 24,543–24,565, doi: 10.1029/98JB00765.

Vigne, G., 1842, Travels in Kashmir, Ladak, Iskardo, the countries adjoining the mountain-course of the Indus, and the Himalaya, north of the Punjab: London, H. Colburn, p. 462.

Zhang, P., Shen, Z., Wang, M., Gan, W., Burgmann, R., Molnar, P., Wang, Q., Niu, Z., Sun, J., Wu, J., Sun, H., and You, X., 2004, Continuous deformation of the Tibetan Plateau from global positioning system data: *Geology*, v. 32, p. 809–812, doi: 10.1130/G20554.1.

Manuscript received 3 July 2006

Revised manuscript received 10 October 2006

Manuscript accepted 29 October 2006

Printed in USA